New class of squalene-based releasable nanoassemblies of paclitaxel, podophyllotoxin, camptothecin and epothilone A

New class of squalene-based releasable nanoassemblies of paclitaxel, podophyllotoxin, camptothecin and epothilone A

Stella Borrelli,[a] Michael S. Christodoulou,[a] Ilaria Ficarra,[a] Alessandra Silvani,[a] Graziella Cappelletti,[b] Daniele Cartelli,[b] Giovanna Damia,[c] Francesca Ricci,[c] Massimo Zucchetti,[c] Franco Dosio,[d*] Daniele Passarella[a*]

[a]*Dipartimento di Chimica - Università degli Studi di Milano - Via C. Golgi 19, 20133 Milano, Italy*
[b]*Dipartimento di Bioscienze - Università degli Studi di Milano - Via Celoria 26, 20133 Milano, Italy*
[c]*Department of Oncology – IRCCS-Istituto di Ricerche Farmacologiche Mario Negri – Via La Masa 19 – 20156 Milano, Italy*
[d]*Dipartimento di Scienza e Tecnologia del Farmaco – Via Giuria 9 – 10125 Torino, Italy*

[*]Corresponding author:
Tel.: +39 02.50314081; fax: +39 02.50314078; E-mail address: daniele.passarella@unimi.it (D. Passarella); Via C. Golgi 19, 20133 Milano, Italy.

Abstract: The present study reports the preparation of a novel class of squalene conjugates with paclitaxel, podophyllotoxin, camptothecin and epothilone A. The obtained compounds are characterized by a squalene tail that makes them able to self-assemble in water, and by a drug unit connected via a disulfide-containing linker to secure the release inside the cell. All the obtained compounds were effectively able to self-assemble and to release the parent drug in vitro. Disulfide containing paclitaxel-squalene derivative showed a similar biological activity when compared to the free drug. Immunofluorescence assay shows that this squalene conjugate enters A549 cells and stain microtubule bundles. The results described herein pave the way for different classes of squalene-based releasable nanoassemblies.

Keywords: Squalene derivatives, nanoassemblies, paclitaxel, podophyllotoxin, camptothecin, epothilone A

1. Introduction

In the treatment of cancer it is often not sufficient to find highly active molecules. The majority of active compounds have its primary target within cells and tissues and, in order to exploit the pharmacological activity, a minimum concentration is needed to be reached at the site of action. Many factors may cause a decrease in the intracellular drug concentration. Among them, we enumerate low water solubility, low partition coefficient across cell membranes and extensive exportation via efflux transporters such as multi-drug resistance proteins and P-glycoproteins. For these reasons, a selective delivery of drugs to their sites of action could result in greater therapeutic effects and potentially minimize side-effects. In recent years, the design, synthesis and application of nanotechnology[1] has opened up new perspectives for biological and biomedical applications[2]. The vasculature in tumor tissues is leaky to macromolecules, having large junctions between the cells. So, nanoparticles can be preferentially delivered to the tumor site thanks to the enhanced permeation and retention (EPR) effect,[3-5] whereas the lymphatic system is usually deficient. In addition to that, nanotechnologies can improve drug properties in several ways: by controlling release and distribution, by enhancing drug absorption by mucosa or cells and by protecting the drug from degradation. Therefore, they offer many possibilities of improving the specificity of drug treatment. Despite this, there is still no universal platform suitable for the delivery of all kinds of drugs, and current nanotechnologies have important limitations.

A great challenge comes from the difficulty to design synthetic materials which combine: a) low toxicity, b) lack of immunogenicity and biodegradability, and c) do not accumulate in cells or tissues.[6] The concept of lipid-drug conjugates has gained considerable attention in recent years, and they are usually obtained by a covalent coupling of the drug to biocompatible lipid moieties. Among them, squalene, a natural precursor of many steroids, showed the ability, when linked to biologically active compounds, to achieve a spontaneous formation of nanoassemblies in water. Thus, squalene, protects the drugs from environment damaging factors and, in some cases, also

improves their pharmacokinetic profile by decreasing the toxicity of the associated drugs with an increase in their therapeutic index.[7] This novel approach progressively extended its field of application from anticancer agents (gemcitabine, paclitaxel, cis-platin, doxorubicin)[6-8] to antibiotics and from antiviral agents (penicillin, AZT, acyclovir)[9,10] to nucleotides (siRNA).[11,12] Furthermore, the ability to spontaneously nanoassemble allowed the preparation of nanoparticles containing both therapeutic and diagnostic agents.[13,14] One of the key points in the realization of potent and efficient squalene prodrug resides in the release of the free drug; thus, the role of the linkage between the drug and the squalene moiety is crucial. Recently, we have demonstrated, in paclitaxel derivatives, the relevant influence of the linker in the cytotoxicity.[6a] Our continuous interest in the field of the synthesis of anticancer compounds[15-18] made us embark on the preparation of squalene-incorporating derivatives with the use of a disulfide containing linker to secure the nanoassemblies and drug release. We reported in different papers the ability of disulfide-containing bivalent compounds to release active drugs inside tumor cells[19] and, on the basis of the results obtained, we envisioned the possibility to prepare a novel class of disulfide-containing squalene conjugates (Scheme 1). The presence of the squalene tail induces spontaneous self-assembly in water, while the disulfide bond induces drug release in the intracellular environment.

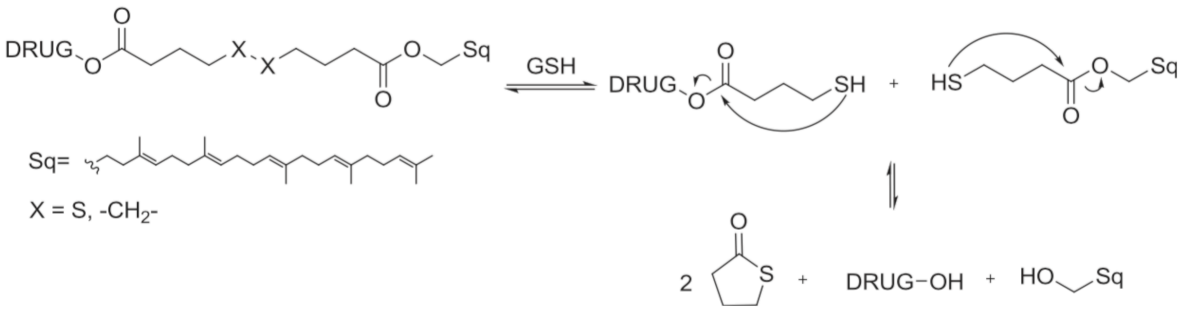

Scheme 1: Supposed pathway for drug release of disulfide-containing squalene conjugates

We selected four known anticancer compounds (Figure 1): paclitaxel, podophyllotoxin, camptothecin and epothilone A. These compounds are known to interact with tubulins (paclitaxel, podophyllotoxin and epothilone A) and with topoisomerase I (camptothecin), but they all suffer

from many drawbacks, primarily due to the side effects associated with their low water solubility. The introduction of a liphophilic tail overcomes the problem by favoring the formation of nanoassemblies, more capable of membrane permeation.

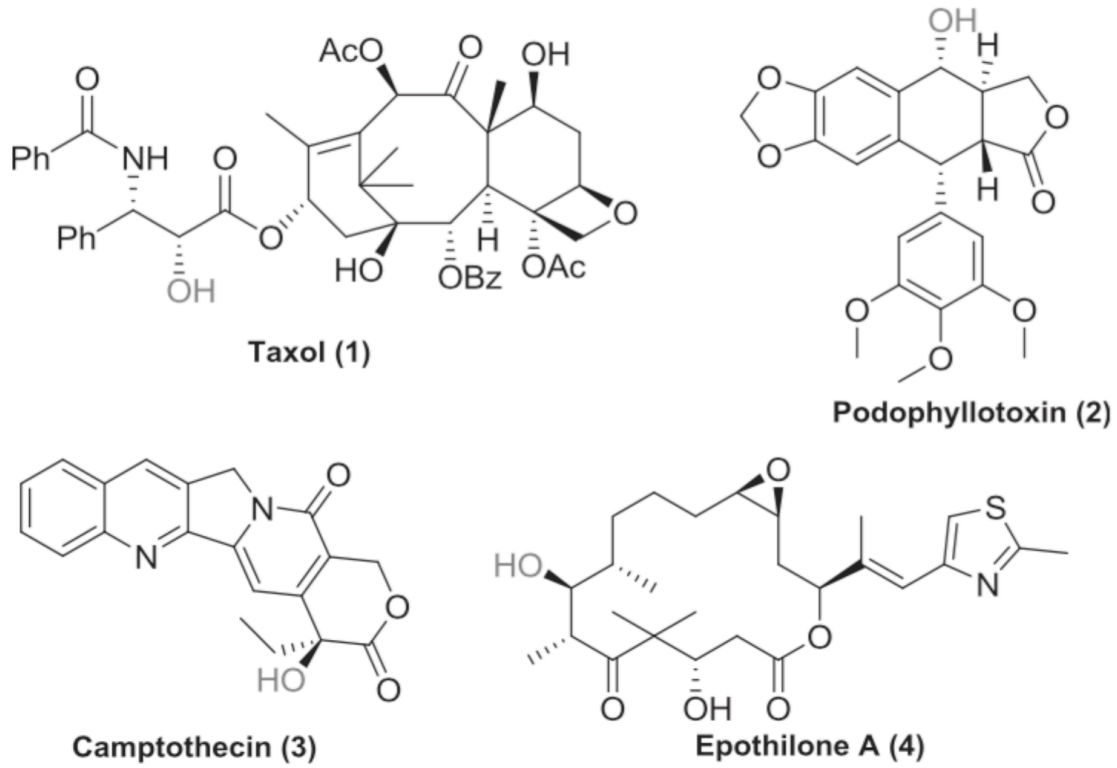

Figure 1: Paclitaxel (**1**), Podophyllotoxin (**2**), Camptothecin (**3**) and Epothilone A (**4**), in red the anchor points.

We describe the synthesis of the conjugates (Scheme 2), the characterization of the nanoassemblies, their ability to release the drug unit, and a preliminary evaluation of their biological activity in vitro.

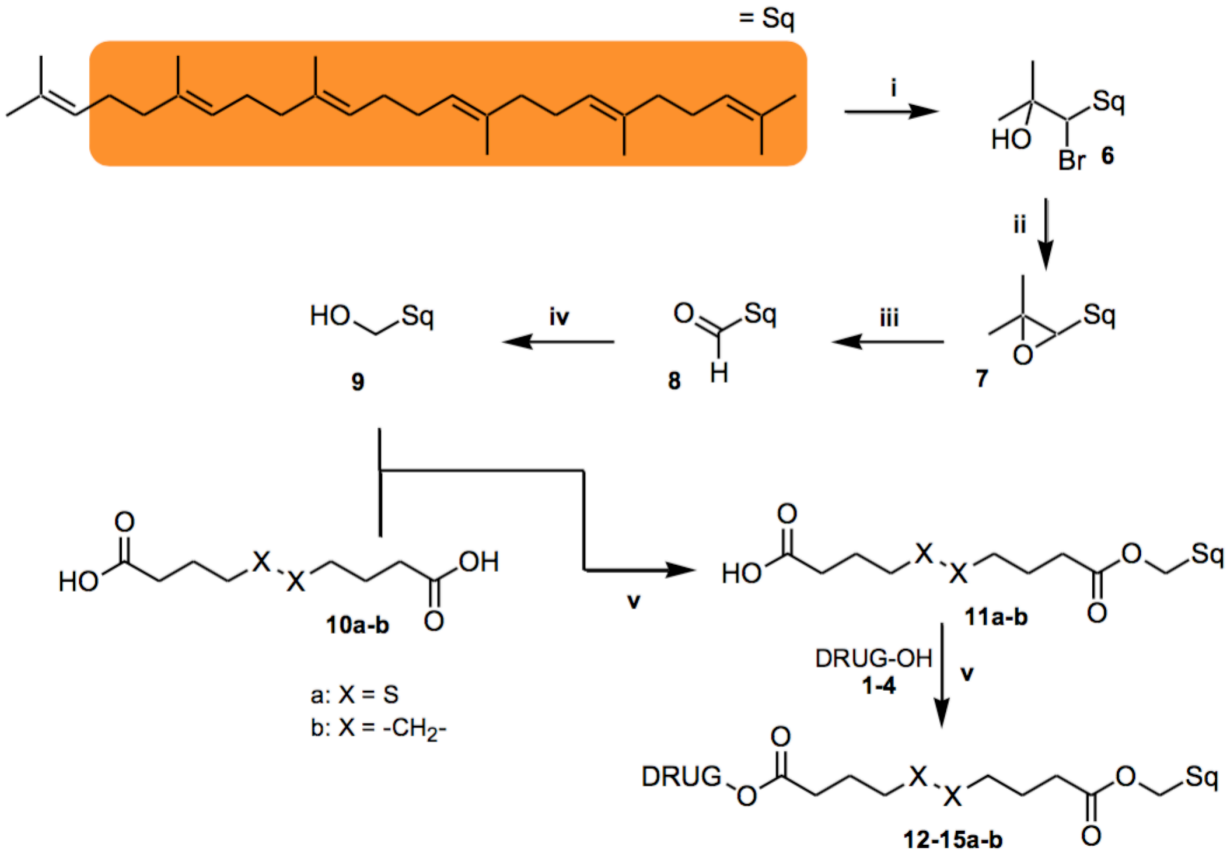

Scheme 2: i) NBS, H_2O, THF; ii) K_2CO_3, MeOH; iii) H_5IO_6, MeOH; iv) $NaBH_4$, MeOH; v) EDC·HCl, DMAP, CH_2Cl_2.

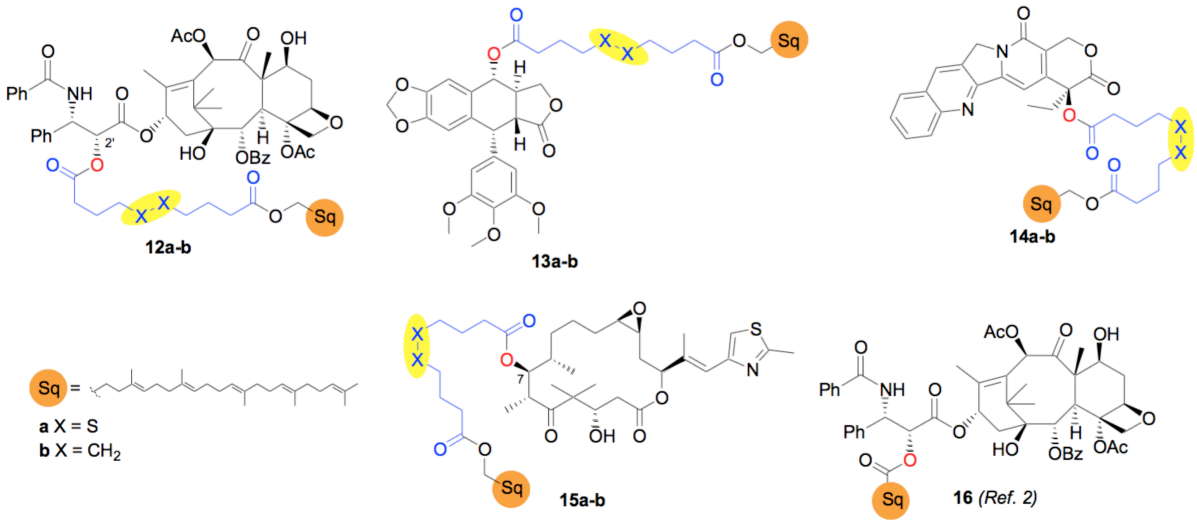

Figure 2: Chemical structures of the obtained conjugate compounds

2. RESULTS AND DISCUSSION

The squalenoylation platform discovered by Couvreur *et al.*[6-8] was employed to design self-assembling nanomedicines of both hydrophilic and hydrophobic therapeutic agents. In this work we explore the efficacy of modifying four hydrophobic anticancer drugs by introducing a squalene-type chain using a labile linker. A novel class of squalene conjugates characterized by a labile disulfide bond has been prepared and characterized. Also, their ability to self-immolate[23] and to release the parent drug has been verified.

2.1. Synthesis of drug-squalene conjugates

A divergent approach has been used. In particular, 1,1',2-tris-norsqualene alcohol was obtained starting from squalene, as described in Scheme 2. The crucial reaction is the formation of monobromohydrine **6** that was converted into 2,3-epoxide **7** by simple treatment with K_2CO_3. The oxidative cleavage of the epoxide furnished 1,1',2-tris-norsqualene aldehyde **8**[24] and the subsequent $NaBH_4$ reduction secured the alcohol **9.** Condensation with dicarboxylic acids **10a-b** gave the corresponding monoesters **11a-b**. These key intermediates were coupled with four different active drugs **1-4**, thus generating a small collection of squalene conjugates. As for paclitaxel and epothilone A conjugates, the regioselectivity of the acylation reaction was assessed on the basis of ^{1}H-NMR spectra of the final compounds. In fact, after the formation of the ester bond, the peak of the proton 2' (paclitaxel) and 7 (epothilone A) respectively is shifted to lower fields. Paclitaxel esters derived from acylation of C2'-OH have been demonstrated to efficiently release paclitaxel.[25] The purity of the obtained compounds was evaluated by HPLC.

2.2. Nanoassemblies: preparation and characterization

Although several articles on squalenoyl NAs are reported, a detailed evaluation of the role of different variables involved in the solvent-displacement precipitation are not yet totally studied. For this reason, a detailed formulation study was carried out just maintaining constant the kind of

solvent able to dissolve up to 8 mg/mL from each compound. We considered as reference the 'standard procedure' applied by several authors for a variety of compounds (2 mg/mL concentration in solvent/water 1:2). The values of size are reported in Table 1. The parameter of size, standard error and polydispersity, monitored by DLS, allowed checking the role of the different variables: volume of solvent, volume of water, final concentration, ionic strength, pH and variety of salt. For all the compounds, the role of volume of the solvent (added up to 1.5 mL to 1 mL of water) was not relevant and the values reported in Table 1 as size and polydispersity index did not range more than 20%. Only for paclitaxel-based compounds (**12a**, **12b**) a size increase of 50% was observed. Increasing the final concentration to 4 mg/mL lead to a significant decrease of size for **14a**, **14b** (to 103.5 nm and 110.6 nm respectively) and **13a** and **13b** (115.6 and 126.5 nm). No differences in size were seen when increasing the ionic strength to 10 mM, but for most of the compounds, the increase to 100 mM tended to cause a rapid size increase and, in some cases, a precipitation of the compound (**12a**, **12b**, **13a**, **13b**). These data are reported in Table 2 together with the data obtained regulating the pH value and buffers. To reduce the variability, three pH values were selected: 4.5 (for acetate and citrate buffers), 7.5 for phosphate and 10.2 for borate and carbonate buffers.

Table 1. Physico-chemical characterization and stability of squalenoyl-drug nanoassemblies

Compound	SIZE[a] (nm)	PI[a]	Z potential[a] (mV)	CAC[b] (mg/l)	NAs stability[c] *(size)*	Comp. stability[d] *(% unaltered)*	NAs stability *(GSH)*[e]
12a	103.2±0.7	0.052	-37.56±7.7	1.5	106.5±1.1	93 ±3	110.5±6.5
12b	107.0±0.1	0.049	-20.78±3.5	1.1	110.5±3.4	95 ±5	120.2±5.7
13a	184.3±2.4	0.063	-11.42±1.7	0.7	215.3±5.1	52 ±2	222.1±12.0
13b	179.6±1.1	0.048	-28.47±2.3	0.5	210.5±7.7	82 ±5	185.3±2.7
14a	195.2±6.8	0.083	-41.02±4.1	1.5	210.2±3.1	70 ±2	234.4±13.5
14b	154.8±7.0	0.279	-39.14±9.2	1.8	172.4±1.2	85 ±8	162.6±3.5
15a	161.6±6.8	0.090	-56.37±2.4	0.6	191.1±2.7	58 ±6	720.5±21.2
15b	124.1±2.5	0.131	-25.39±4.37	0.8	142.9±4.7	70 ±8	130.3±8.1
16	173.5±3.9	0.030	-34.62±2.7	0.2	181.1±10.7	94 ± 4	195.4±3.2

All formulations were prepared using nanoprecipitation technique at a concentration of 2 mg/mL aqueous nanodispersions.
[a)] Particle mean diameter, polydispersity index (P.I.) and charge, were determined using a Brookhaven Nanosizer. [b)] Critical aggregation concentration (CAC) measurement by pyrene was obtained from a ratio between I373 and I384 as a function of concentration. [c)] Stability was assessed by measuring the size of samples diluted with water (checked after three months at 5°C). [d)] Stability was assessed by evaluating the ratio of HPLC area of peaks corresponding to intact compounds at T=0 and after incubation with human serum at 37°C for 48h. [e)] Stability was assessed by measuring the size of samples of NAs exposed to 10 mmol/L GSH for 24 h.

Acidic pH (citrate buffer, table 2) induced an increase of the NAs (from 200 nm to 1 μm) while acetate buffer destabilized only the paclitaxel derivatives **12**. The phosphate buffer and neutral pH allowed obtaining NAs with size very close to that obtained in water. At basic pH values (10.2) some compounds were unstable, for example the epothilone derivatives **15,** NAs rapidly turned to brown color with both buffers, while carbonate buffer lead to an effective increase of size for almost all bioconjugates (from 212 to 600 nm). The preparation in water (phosphate buffer pH 7.2 or 10 mM NaCl), lead to the smallest NAs which did not present signs of size increase over time. The studied molecules do not contain any ionizable group and, for this reason, the different behavior of some buffers citrate vs acetate, carbonate vs borate seems directly due to the squalene-type component of NAs. No significant differences in stability for disulfide vs alkyl derivatives were observed in these tests.

Table 2. NAs preparation: role of pH, buffer and ionic strength

NAs from compounds								
Water/buffer	**12a**	**12b**	**13a**	**13b**	**14a**	**14b**	**15a**	**15b**
Water	100.8±1.2	107.9±2.3	185.9±8.2	180.5±9.3	195.3±7.9	160.2±5.1	165.1±4.7	125.3±3.5
Citrate pH 4.5	462.4±71.2	391.2±31.4	428.3±29.1	629.2±81.3	376.4±9.6	375.4±12.1	197.8±9.2	203.2±8.6
Acetate pH 4.5	>2 μm	>2 μm	275.9±9.3	287.5±7.1	224.3±11.2	275.9±21.3	201.5±5.2	206.0±13.7
Phosphate pH 7.5	162.4±10.3	125.60±9.3	201.5±14.0	193.5±8.4	198.9±9.3	201,5±13.1	235.5±15.6	212.9±23.9
Borate pH 10.2	181.7±14.0	161.4±11.2	202.3±9.9	211.3±15.2	160.3±9.7	202.3±11.9	207.7±15.2[a]	351.1±23.2[a]
Carbonate pH 10.2	723.3±34.2	635.9±52.2	242.9±18.9	315.0±19.3	250.6±11.2	242.9±20.0	212.2±19.2[a]	312.2±22.1[a]
NaCl 100 mM	>2 μm	>2 μm	676.0±44.2	720.3±33.7	339.7±9.8	461.1±15.2	312.9±23.5	502.4±41.32

The table shows the size of NAs obtained using water or different buffers (10 mM) and at different pH values and ionic strength (due to buffer and sodium chloride) in the solvent displacement process (final concentration 2 mg/mL). [a)] brown colour appeared.

Taking into account the preparation in water at a standard concentration of 2 mg/mL these aqueous NA suspensions were found to be physically stable (by measure of particle size) for months when stored at 4°C (Table 1). NAs deriving from paclitaxel appeared smaller than NA-**16** while no significant differences in size were seen evaluating different disulfide of alkylic chain. This unique ability of the squalene-derivatives to form NAs in water was further confirmed by the critical aggregation concentration (CAC) measurement. It has to be noted that the observed CAC values were higher than compound **16**[6] but still lower than those of polymeric micelles used for drug delivery purposes (5-10 mg/L). Moreover, the size of the NAs of all the conjugates remained unchanged upon dilution into water (data not shown).

2.3. Stability of squalene-derivatives and NAs

The stability of NAs was initially evaluated using the same conditions as in the preparations step, in order to compare the role of pH and buffer type in preformed NAs. Figure 3 represents the NAs size after dilution in buffers and sampled after different times. For all compounds, except those

derived by paclitaxel, the citrate buffer tended to increase the size after one day. Paclitaxel compounds demonstrated immediate instability in carbonate buffer, with an almost complete precipitation after 24 h. However, no instability was observed in borate buffer, at the same pH value. NAs from epothilone A (15a and b) showed high instability, and after 1 h, in all conditions, a significant increase in size and a color brown appeared. In basic conditions, NAs of compound **14a** (camptothecin), but not **14b**, increased in size.

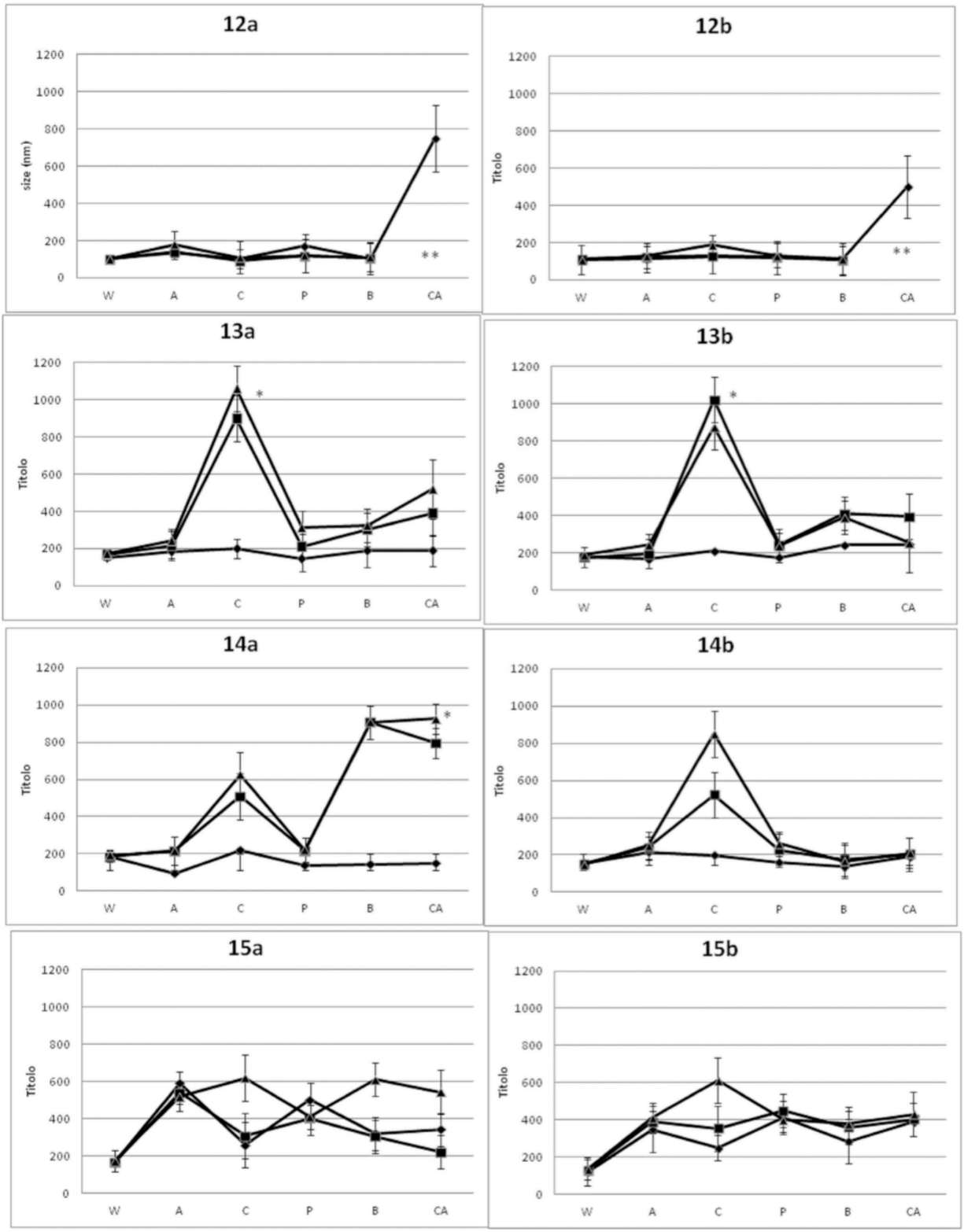

Figure 3. Size measurement (expressed in nm) of NAs diluted in water (W), C, citrate buffer 10 mM pH 4.5; A, acetate buffer 10 mM pH 4.5; P, phosphate buffer 10 mM pH 7.5; B, borate buffer 10 mM pH 10.2; CA, carbonate buffer 10 mM pH 10.2. after 1 (diamond), 24 (square) and 48 hours (triangle) at 20°C. No correct detection was observed ** due to precipitation, while a reduction of turbidity was represented by *.

Contrary to the results of formulation, dilution of preformed NAs ,for all the compounds, in 100 mM NaCl did not significantly improve their size.

In order to investigate the chemical stability of disulfide containing squalene-drug both as compound in solution and as assembled in nanostructure, samples at a concentration of 1 mg/ml were incubated at a pH 8 with a final concentration of 0.54 mM of the reductive agent dithiotreitol (DTT). Using appropriate volume of acetonitrile/water it was possible to avoid the NAs formation also allowing complete solubility of DTT. The chemical stability of the disulfide bond was determined by monitoring the peak of the squalene derivatives. Figure 4 demonstrates the appearance of the free drug after treatment of **12a** with DTT.

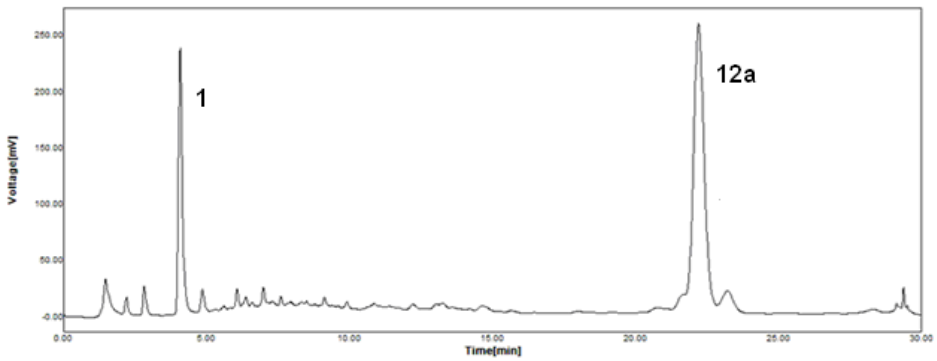

Figure 4: Example of HPLC analysis for compound **12a** (in acetonitrile) after 1h incubation with DTT.

Figure 5 shows the results of derivatives with disulfide bonds. In panel A, the size of NAs after exposure of DTT is represented (up to 78 h), while panels B-E represent the release/degradation of the compounds (as NAs or soluble compounds) as detected by HPLC analysis. For all the disulfide linked compounds the buffer alone did not significantly influence the stability of disulfide bond or the ester linkage for compounds **12b**, **13b**, **14b**, **15b** (data not shown). After addition of DTT, a rapid break of the disulfide bond was evident only for the compounds dissolved in organic solvent. All NAs when treated with DTT appeared stable with very slow release of drug during the first two days. A correlation between stability of NAs and inner

component seems to appear for podophillotoxin derivative **13a,** and in a minor percentage for epothilone **15a**, where NAs instability also produced a fast disulfide release. Further compounds characterization were carried out by incubation NAs in human serum for two days at 37°C (Table 1). NAs showed good stability but an increased release for all the disulfide linked compounds appears evident. Paclitaxel derivatives were the most stable while significant release occurred for podophyllotoxin and epothilone derivatives (around 48-42% released after 48h). Furthermore, also glutathione was used to monitor the stability of NAs. Indeed cancer cells express high levels of detoxifying enzymes such as glutathione-S-transferases (GSTs) and glutathione (GSH) to protect themselves from toxic xenobiotics. In our case the NAs were exposed to the presence of 10 mmol/L GSH (corresponding to an intracellular level) for up to 24h. For compounds **12a**, **13a**, **14a** (Table 1) a progressive slight increase of size was evident while for NA-**15a** the size increased dramatically and precipitation occurred. Both DTT and GSH treatments did not significantly modify the stability and morphology of NAs of compounds **12b**, **13b**, **14b**, **15b.**

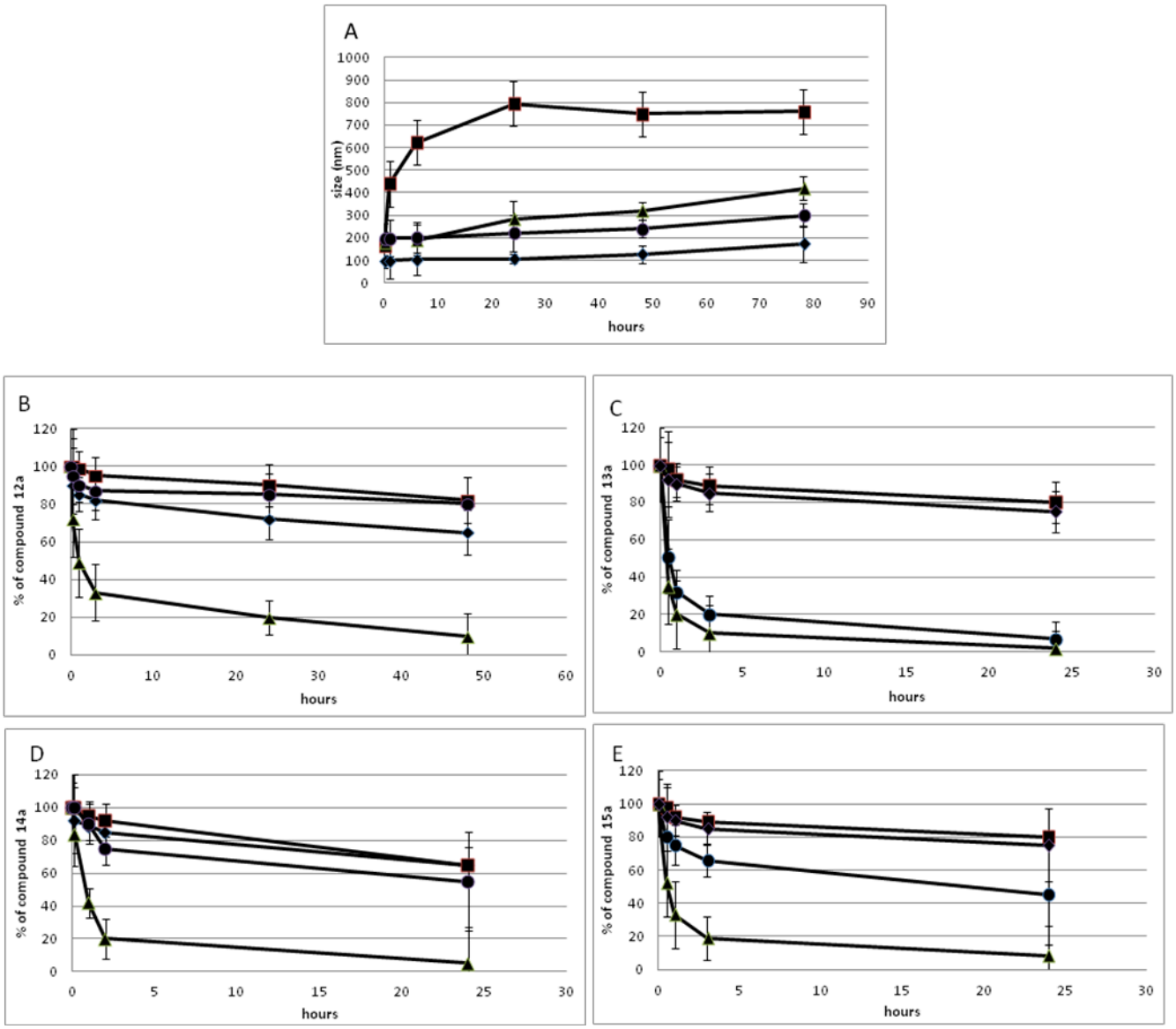

Figure 5: Stability of disulfide-linked squalene derivatives and NAs by incubation in medium plus DTT. A) size measure of the NAs obtained from compounds **12a** (diamond), **13a** (square), **14a** (circle), **15a** (triangle). B-E) release percentage for compounds **12a**, **13a,14a, 15a** respectively when maintained as native compound (diamond) in solvent+buffer, as NA in buffer (square), as native compound in the presence of DTT (triangle) and as NA in the presence of DTT (circle).

2.3.1 Atomic force microscopy characterization.

The morphology of NAs was investigated by Atomic force microscopy (AFM). A topography AFM image and the related 3D reconstruction of compound 13a, as reference, is presented in Figure 6. As evident from the images, spherical soft structures with a certain degree of

aggregation appeared. It is relevant to notice that AFM technique, even if in non contact mode, deform the soft structure of NAs due to the interaction between the sample and the substrate, and the vertical force applied by the tip on the sample during the scanning procedure. Indeed, it was observed that only using 10 mM NaCl instead of pure water in NAs preparation, (checking the QELS scattering intensity value of 700-800 kcps for a 0.2 mg/ml sample) a stable signals were obtained for all the NAs.

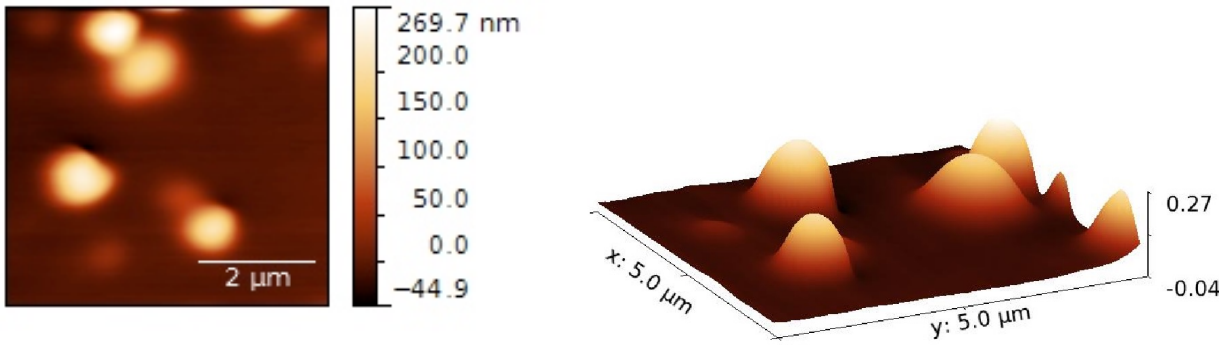

Figure 6: AFM images by non-contact mode of **13a** nanoassemblies after sample deposition on mica support: topography on the top, and 3D-view.

2.4. Microtubule bundle formation (immunofluorescence)

In order to confirm the anti-microtubule effect deriving from the use of squalene bioconjugates, by the staining of one of the building elements of microtubules (i.e. α tubulin, α-TUB), we investigated their structure and distribution in A549 cell line exposed 1h to the conjugates **12a**, **13a** and **15a** (200 µg/ml) or to equal concentration of parent naive drugs (**1**, **2** and **4**). Microscopy analyses reveal that control cells are spread with a well-organized microtubular network, whereas treated cells are shrinking and no obvious differences following incubation with naïve compounds and squalene conjugates are noticeable (Figure 7). As expected, paclitaxel and epothilone-A induce microtubule bundling; on the other hand, podophyllotoxin completely disrupts microtubules. Furthermore, in the presence of both naïve and squalene conjugate compounds, there are some detaching cells, as highlighted by their roundish morphology, due to the heavy impact of the compounds on microtubule reorganization (Figure 8). To verify that the observed effects were due

to intracellular action of the NA squalene conjugates we verified (at least for NA-12a) that NAs had retained the ability to cross the cell membrane and probably to release the native drug (in this case paclitaxel). Therefore, we removed all the unassembled tubulin, leaving only the polymerized one (i.e. microtubules) and the molecules tightly bound to the microtubules. As showed in figure 9, microtubule bundles (arrows) are well decorated with anti-taxol antibodies in cells treated with naïve paclitaxel and with NA-12a as well, proving that squalene conjugate paclitaxel enters the cells and exerts its effects through the action on microtubule cytoskeleton.

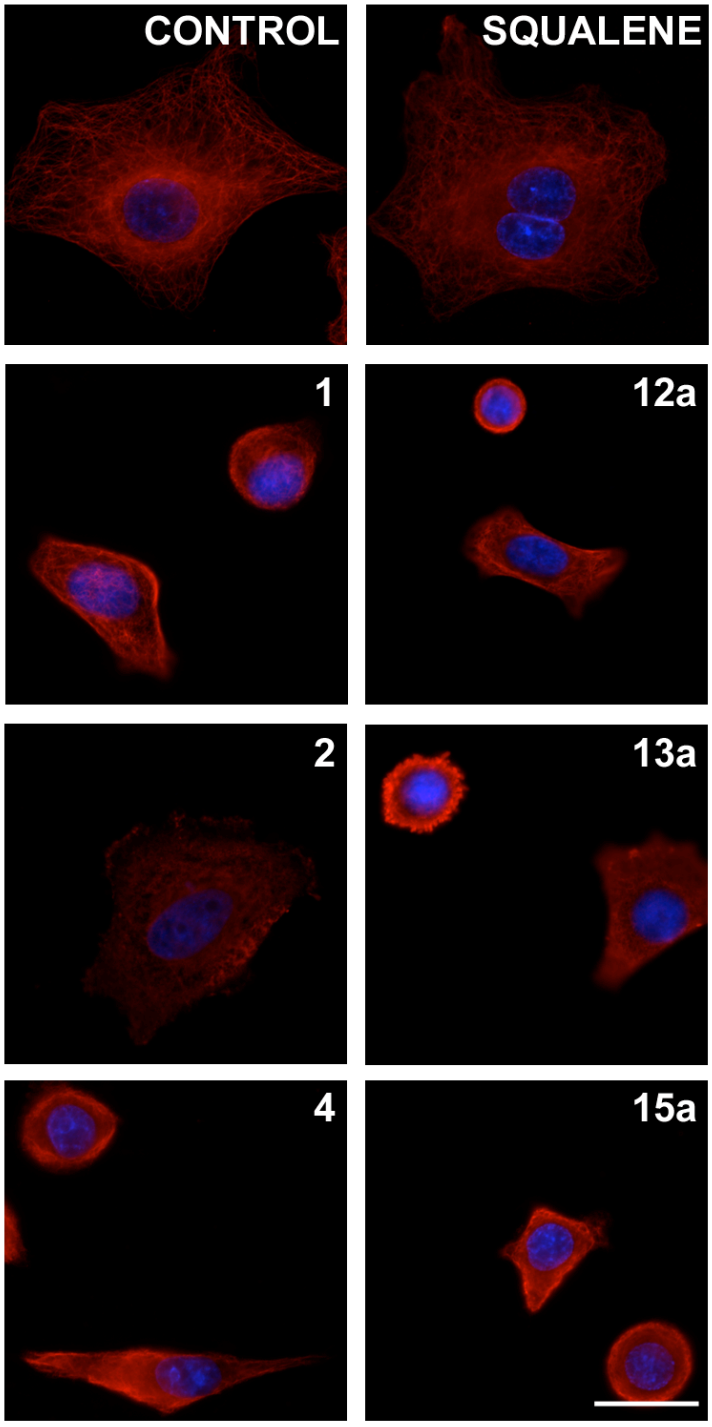

Figure 7: Microtubule network (α-TUB staining, red) and nuclei (DAPI, blue) of A549 cells not loaded (CONTROL) or incubated 1h with squalene (SQUALENE) or with naïve compounds (1, 2, and 4) or squalene bioconjugates (12a, 13a and 15a). Scale bar = 20 μm

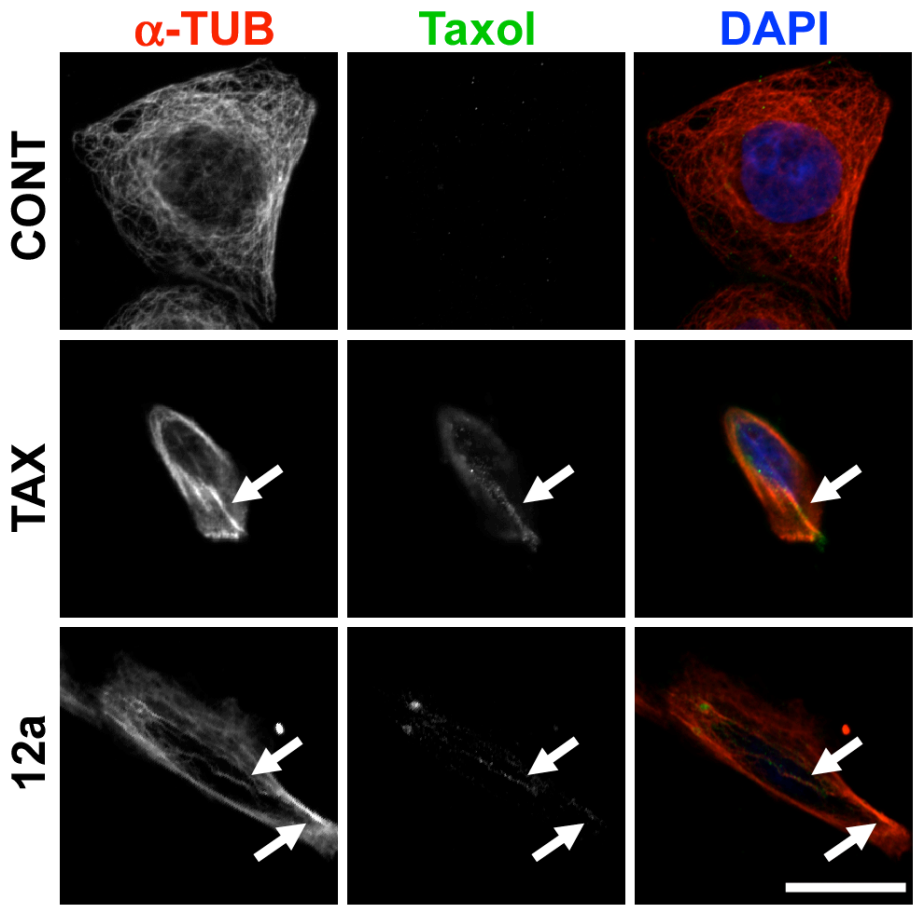

Figure 8: Microtubule network (α-TUB, red), microtubule-bound taxol (TAX, green) and nuclei (DAPI, blue) of A549 cells not loaded (CONT) or incubated 1h with naïve paclitaxel (TAX) or NA-12a (**12a**). Arrows indicate microtubule bundles decorated by anti-paclitaxel antibody. Scale bar = 20 μm

2.5. In vitro activity

The cytotoxicity of squalene conjugates (NAs) was evaluated using MCF7 cell line by incubation for 48 h (Table 3). In order to check the release ability by the reducing agent the same experiments were carried out after NAs treatment with DTT (10 mM). Comparison of the dose-response curves obtained for each drug and squalene conjugates NAs, revealed that the conjugation to squalene decreased the cytotoxicity toward MCF7 cell line for each compound (Table 3). Even if MCF7 seems very sensitive to single drug (in nano and sub-nanomolar range), the various squalene conjugates exhibited different IC_{50} values. Paclitaxel derivative **12a** appeared 100 times more toxic than the **13a**, whilst the podophillotoxin is the most active free drug, indicating that there is no direct correlation between cytotoxicity of free drug and those of conjugates. In a scale of activity we can place **12a > 13a > 15a > 14a**. When comparing the disulfide derivatives with the alkyl chain

ones, we observed that the presence of the disulfide bond makes the release of the toxic moiety more efficient.The alkyl chain derivatives were active only at very high concentrations, ranging from 1 to 100 micromolar.

The incubation of NAs **12a, 13a, 14a** with DTT, allowed a better release of the active molecule as detected by a tenfold increase of activity. In particular compound **12a** reached an activity similar to that of the free paclitaxel. The treatment with the thiol reducing agent did not significantly change the activity of **12b, 13b,** and **14b** as it did for the corresponding NAs.

The disulfide compounds **12-15a** were evaluated also against A549 cell line. Paclitaxel derivative **12a** presents the best performance and resulted 7 times less active than paclitaxel.

Table 3: cytotoxicity of squalene conjugates and naïve compounds against MCF7 and A549. Squalenoyl-taxol **16** has been used as reference compound. Dose-response curves of **12a** and paclitaxel in A549 cell line.

	IC_{50} (μM) MCF7	IC_{50} (μM) MCF7 (DDT)	IC_{50} (μM) A549
12a	0.06 ± 0.01	0.003 ± 0.001	0.49 ± 0.07
12b	1.21 ± 0.21	1.53 ± 0.09	-
1	0.004 ± 0.001	0.005 ± 0.002	0.082 ± 0.0498
16	9.1 ± 0.19	8.7 ± 0.08	-
13a	0.4 ± 0.11	0.06 ± 0.005	7.64 ± 0.33
13b	105.5 ± 4.8	110.8 ± 5.6	-
2	0.0001 ± 0.00006	0.0004 ± 0.0001	0.059 ± 0.0028
14a	8.6 ± 0.1	0.8 ± 0.07	>5
14b	10.5 ± 1.3	20.1 ± 0.8	-
3	0.0005 ± 0.0001	0.003 ± 0.0005	1.3 ± 0.37
15a	1.3 ± 0.2	0.5 ± 0.08	>5
15b	40.2 ± 2.8	45.1 ± 1.7	-
4	0.0009 ± 0.0001	0.0008 ± 0.0002	>5

3. Conclusions

A class of squalene-based conjugate compounds of paclitaxel, podophyllotoxin, camptothecin and epothilone A were prepared. The obtained compounds self-assemble and form nanoassemblies that we characterized in this study. We demonstrated that from all the NAs only paclitaxel-derivative **12a** shows moderate release when treated with glutathione, dithiotreitol and serum. On the contrary all the non-NA forms of compounds **12-15a** present excellent release of the corresponding drug. The in vitro activity highlights the importance of the disulfide bond. The capacity to permeate the cell membrane was indirectly demonstrated for compound **12a** by studying the microtubule structure and distribution in A549 cell line. The results acquired from the **12-15a** derivatives can be a starting point for constructing nanoassemblies bearing a disulfide bridge.

4. Experimental part

4.1. Chemistry. General methods

Thin layer chromatography (TLC) was performed on Merck precoated $60F_{254}$ plates. Reactions were monitored by TLC on silica gel, and detected by I_2 and by UV light (254 nm) accordingly. Flash chromatography was performed using silica gel (240-400 mesh, Merck). ^{1}H NMR and ^{13}C NMR spectra were recorded at 400, 300 and 100, 75 MHz respectively on Bruker DRX-400 and DRX-300 spectrometers in the indicated solvents. Chemical shifts (δ) for proton and carbon resonances are quoted in parts per million (ppm) relative to tetramethylsilane (TMS), which was used as an internal standard. APCI mass spectra were recorded at a Thermo Fischer instrument.

ESI mass spectra were recorded on Thermo Fischer Finningan LCQ Advantage Mass Spectometer and on FT-ICR APEX^{II} (Bruker Daltonics). Quasi-elastic light scattering (QELS) and zeta potential measurements were carried out using a 90 Plus Particle Size Analyzer (Brookhaven Instruments, Co.) photometer. HPLC analysis: RP-18 reverse phase column (LiChrospher 100 RP 18e 5 μm, Merck).

4.1.1. Synthesis of 2-Hydroxy-3-bromosqualene (**6**)

To a solution of Squalene (4.290 g, 10.4 mmol) in THF (30 ml) H_2O (5 ml) is added and then THF dropwise to obtain a clear solution. N-bromosuccinimide (2.231 g, 12.5 mmol) is added portionwise and the reaction mixture is stirred at room temperature for 3h. the solvent is removed under reduced pressure, brine (100 ml) is added and extracted with AcOEt (5x20 ml). The organic layers are dried over Na_2SO_4 and the solvent is removed under reduced pressure. The crude is purified by flash chromatography (CH_2Cl_2:Hex 1:1) to obtain **6** as a pale-yellow oil (1.652 g, Yield: 31%). ^{1}H-NMR ($CDCl_3$, 400 MHz): δ(ppm)= 5.10-5.25 (m, 5H); 4.01 (dd, J = 11.3 Hz, J = 1.9 Hz, 1H); 2.32-2.35 (m, 1H), 1.95-2.17 (m, 18H); 1.77-1.88 (m, 1H); 1.70 (s, 3H); 1.63 (bs, 15H); 1.37 (s, 3H); 1.36 (s, 3H). ^{13}C-NMR ($CDCl_3$, 100 MHz): δ(ppm)= 135.1; 134.8; 132.9; 131.2; 126.0; 124.5; 124.3 (3C);

72.4; 71.0; 39.7 (3C); 38.2; 32.2; 28.3 (3C); 26.7 (2C); 25.8 (3C); 17.7; 16.0 (3C); 15.8. APCI-MS: m/z 507.3 $[M]^+$.

4.1.2. Synthesis of 2,3-oxidosqualene (**7**)

To a solution of **6** (1.652 g, 3.2 mmol) in MeOH (60 ml) K_2CO_3 (0.898 g, 6.5 mmol) is added and the reaction mixture is stirred at room temperature for 2 h, then concentrated under reduced pressure. H_2O (120 ml) is added and extracted with AcOEt (4x30 ml). The organic layers are dried over Na_2SO_4 and the solvent is removed under reduced pressure to obtain **7** as a yellow oil (1.360 g, Yield: 98%) without any further purification. ^{1}H-NMR ($CDCl_3$, 300 MHz): δ(ppm)= 5.06-5.17 (m, 5H); 2.69 (t, *J* = 6.1 Hz, 1H); 1.95-2.19 (m, 20H); 1.68 (s, 3H); 1.60 (s, 3H); 1.58 (bs, 12H); 1.28 (s, 3H); 1.24 (s, 3H). ^{13}C-NMR ($CDCl_3$, 100 MHz): δ(ppm)= 135.1; 134.9 (2C); 134.0; 131.2; 124.9; 124.3 (4C); 64.2; 58.3; 39.7 (3C); 36.3; 28.2 (2C); 27.5; 25.7; 24.9 (2C); 18.7; 17.7; 16.0 (3C). APCI-MS: m/z 427.3 $[M+1]^+$.

4.1.3. Synthesis of 1,1',2-tris-norsqualene aldehyde (**8**)

To a solution of H_5IO_6 (1.379 g, 6.0 mmol) in H_2O (5 ml) a solution of **7** (1.434 g, 3.4 mmol) in dioxane (12 ml) is added and the reaction mixture is stirred at room temperature for 2h. H_2O (150 ml) is added and extracted with AcOEt (3x40 ml). the organic layers are washed with brine (100 ml) and H_2O (100 ml), then dried over Na_2SO_4 and concentrated under reduced pressure to obtain **8** as a pale yellow oil (1.111 g, Yield: 86%) without any further purification. ^{1}H-NMR ($CDCl_3$, 300 MHz): δ(ppm)= 9.73 (s, 1H); 5.06-5.13 (m, 5H); 2.49 (t, *J* = 7.1 Hz, 2H); 2.30 (t, *J* = 7.1 Hz, 2H); 1.97-2.10 (m, 16H); 1.67 (s, 3H); 1.55 (bs, 15H). ^{13}C-NMR ($CDCl_3$, 75 MHz): δ(ppm)= 202.6; 135.1; 134.9; 134.8; 132.9; 131.2; 125.4; 124.5; 124.4; 124.2 (2C); 67.1; 42.1; 39.7 (2C); 39.5; 31.8; 28.2 (2C); 26.7; 26.6; 25.7 (2C); 17.7; 16.0 (3C). APCI-MS: m/z 385.3 $[M+1]^+$.

4.1.4. Synthesis of 1,1',2-tris-norsqualene alcohol (**9**)

To a solution of **8** (1.111 g, 2.9 mmol) in MeOH (45 ml) $NaBH_4$ (0.055 g, 1.4 mmol) is added portionwise and the reaction mixture is stirred at room temperature for 1 h. HCl 1M is added to quench the unreacted $NaBH_4$. The solvent is the removed under reduced pressure, H_2O (150 ml) is added and extracted with AcOEt (3x40 ml). the organic layers are dried over Na_2SO_4 and concentrated under reduced pressure to obtain **9** as a colorless oil (1.016 g, Yield: 91%) without any further purification. ^{1}H-NMR ($CDCl_3$, 300 MHz): δ(ppm)= 5.08-5.13 (m, 5H); 3.61 (t, *J* = 6.3 Hz, 2H); 1.99-2.08 (m, 18H); 1.78-1.85 (m, 2H); 1.67 (s, 3H); 1.59 (s, 15H). ^{13}C-NMR ($CDCl_3$, 75 MHz): δ(ppm)= 135.1; 134.9 (2C); 134.5; 131.2; 125.8; 124.4 (2C); 124.3 (2C); 62.8; 39.7 (3C); 36.0; 30.7; 28.2 (2C); 26.6 (3C); 25.7 (2C); 17.7; 16.0 (3C). APCI-MS: m/z 387.3 $[M+1]^+$.

4.1.5. General procedure for compounds **11**

To a solution of **9** (0.26 mmol) in dry CH_2Cl_2 (2.5 ml) the bicarboxylic acid **10** (0.52 mmol), EDC·HCl (0.31 mmol) and DMAP (0.18 mmol) are added and the reaction mixture is stirred at room temperature for 24 h. HCl 1M (15 ml) is added and extracted with CH_2Cl_2 (5x5 ml). The organic layers are dried over Na_2SO_4 and the solvent is removed under reduced pressure. The crude is purified by flash chromatography (AcOEt/Hex) to obtain **11** as a colorless oil (Yield: 35-60%).

11a: ^{1}H-NMR ($CDCl_3$, 300 MHz): δ(ppm)= 5.06-5.12 (m, 5H); 4.03 (t, J = 6.0 Hz, 2H); 2.68-2.74 (m, 4H); 2.40-2.51 (m, 4H); 1.99-2.07 (m, 22H); 1.71-1.79 (m, 2H); 1.68 (s, 3H); 1.59 (s, 15H). ^{13}C-NMR ($CDCl_3$, 75 MHz): δ(ppm)= 178.0; 173.1; 135.1; 134.9; 133.6; 125.1; 124.3 (4C); 64.3; 39.7 (3C); 37.8; 37.6; 35.8; 32.6; 32.1; 28.2 (3C); 26.8; 26.7 (3C); 25.7; 24.3 (2C); 23.9; 17.7; 16.0 (3C); 15.9. ESI-MS: m/z 606.2 $[M-1]^+$.

11b: ^{1}H-NMR ($CDCl_3$, 300 MHz): δ(ppm)= 5.06-5.13 (m, 5H); 4.02 (t, J = 9.0 Hz, 2H); 2.25-2.36 (m, 4H); 1.97-2.08 (m, 20H); 1.59-1.84 (m, 22H); 1.30 (bs, 8H). ^{13}C-NMR ($CDCl_3$, 75 MHz): δ(ppm)= 178.9; 173.9; 135.1; 134.9; 1337.7; 125.1; 124.3 (4C); 64.0; 39.7 (3C); 35.8; 34.3; 33.8; 29.7; 29.0 (4C); 28.2 (3C); 26.9; 26.7 (2C); 25.6; 24.9 (2C); 24.6; 17.7; 16.0 (4C). ESI-MS: m/z 507.3 $[M-1]^+$.

4.1.6. General procedure for compounds **12-15**

To a solution of **11** (0.04 mmol), in dry CH_2Cl_2 (1 ml) EDC·HCl (0.06 mmol) and DMAP (0.03 mmol) are added. The drug (0.04 mmol) is added and the reaction mixture is stirred at room temperature for 3-96h. HCl 1M (15 ml) is added and extracted with CH_2Cl_2 (5x5 ml). The organic layers are dried over Na_2SO_4 and the solvent is removed under reduced pressure. The crude is purified by flash chromatography (AcOEt/Hex) to obtain **12-15** as a solid (Yield: 15-70%).

12a: ^{1}H-NMR ($CDCl_3$, 400 MHz): δ(ppm)= 8.17 (d, J = 7.1Hz, 2H); 7.77 (d, J = 7.1 Hz, 2H); 7.63 (t, J = 7.1 Hz, 1H); 7.51-7.56 (m, 3H); 7.35-7.47 (m, 10H); 6.93 (d, J = 9.3 Hz, 1H); 6.32 (s, 1H); 6.28 (t, J = 9.0 Hz, 1H); 6.00 (dd, J = 9.2 Hz, J = 3.1 Hz, 1H); 5.71 (d, J = 7.1 Hz, 1H); 5.53 (d, J = 3.1 Hz, 1H); 5.32 (s, 2H); 5.10-5.16 (m, 5H); 5.00 (d, J = 7.6 Hz, 1H); 4.50 (dd, J = 10.9 Hz, J = 6.6 Hz, 1H); 4.34 (d, J = 8.4 Hz, 1H); 4.23 (d, J = 8.4 Hz, 1H); 4.05 (t, J = 6.7 Hz, 2H); 3.84 (d, J = 7.0 Hz, 2H); 2.51-2.73 (m, 6H); 2.48 (s, 3H); 2.25 (t, J = 7.2 Hz, 2H); 2.25 (s, 3H); 2.15-2.22 (m, 2H); 1.87-2.13 (m, 20H); 1.68-1.79 (m, 8H); 1.63 (bs, 18H); 1.26 (s, 3H); 1.16 (bs, 3H). ^{13}C-NMR ($CDCl_3$, 100 MHz, detected signals): δ(ppm)= 204.5; 173.6; 172.6; 171.9; 170.5; 168.7; 167.8; 143.5; 137.7; 135.8; 135.6; 134.4; 134.3; 133.5; 132.7; 130.9; 129.8; 129.4; 129.2; 127.8; 127.2; 125.8; 125.0; 124.9; 85.1; 81.7; 79.9; 77.1; 76.3; 75.8; 74.7; 72.8; 72.5; 65.0; 59.2; 53.4; 46.3; 43.9; 40.4; 38.4; 37.8; 36.5; 36.3; 33.3; 32.7; 29.0; 27.6; 27.5; 27.4; 26.4; 24.9; 24.6; 23.4; 22.8; 21.5; 18.3; 16.7; 16.6; 15.5. HPLC (CH_3CN) R_f 22 min; ESI-MS ($C_{82}H_{107}NO_{17}S_2$): m/z 1465.8 $[M+Na]^+$. $[\alpha]^{22}_D$ = -46 (c = 0.100, $CHCl_3$).

12b: ^{1}H-NMR (CD_3OD-*d*$_4$, 400 MHz, detected signals): δ(ppm)= 8.14 (d, J = 8.0 Hz, 2H); 7.83 (d, J = 8.0 Hz, 2H); 7.70 (t, J = 7.2 Hz, 1H); 7.44-7.63 (m, 10H); 7.29 (t, J = 7.2 Hz, 1H); 6.48 (s, 1H); 6.09 (t, J = 6.8 Hz, 1H); 5.87 (d, J = 6.4 Hz, 1H); 5.66 (d, J = 7.2 Hz, 1H); 5.11-5.16 (m, 5H); 5.02 (d, J = 8.0 Hz, 1H); 4.37 (dd, J = 11.2 Hz, J = 6.8 Hz, 1H); 4.21 (s, 2H); 4.05 (t, J = 6.8 Hz, 2H);

3.84 (d, J = 7.2 Hz, 1H); 2.43-2.50 (m, 5H); 2.30 (t, J = 8.0 Hz, 2H); 2.19 (s, 3H); 1.99-2.15 (m, 16H); 1.95 (s, 2H); 1.72-1.88 (m, 6H); 1.68 (bs, 6H); 1.63 (bs, 15H); 1.28 (bs, 8H); 1.56 (bs, 6H). ^{13}C-NMR (CD_3OD-*d_4*, 100 MHz, detected signals): δ(ppm)= 203.8; 174.2; 174.0; 170.2; 169.9; 169.1; 166.3; 141.0; 137.0; 134.6; 134.4; 134.2; 133.5; 133.2; 131.5; 130.6; 130.0; 129.8; 128.7; 128.5; 128.3; 128.2; 127.2; 124.9; 124.3; 124.2; 124.1; 84.5; 80.9; 77.7; 76.1; 75.4; 74.9; 74.3; 71.5; 70.9; 63.6; 57.9; 53.9; 46.5; 43.2; 39.4; 39.3; 36.1; 35.5; 35.1; 33.8; 33.2; 28.7; 28.5; 27.8; 26.6; 26.5; 26.2; 26.1; 25.6; 24.7; 24.5; 21.9; 21.0; 19.4; 14.8; 14.6; 13.5; 9.0. HPLC (CH_3CN) R_f 27 min; ESI-MS ($C_{84}H_{111}NO_{17}$): m/z 1429.9 $[M+Na]^+$. $[\alpha]^{22}_D$ = -24 (c = 0.100, $CHCl_3$).

13a: ^{1}H-NMR ($CDCl_3$, 400 MHz): δ(ppm)= 6.79 (s, 1H); 6.57 (s, 1H); 6.42 (bs, 2H); 6.02 (d, J = 1.0 Hz, 1H); 6.00 (d, J = 1.0 Hz, 1H); 5.92 (dd, J = 9.0 Hz, J = 4.0 Hz, 1H); 5.10-5.17 (m, 5H); 4.63 (d, J = 4.2 Hz, 1H); 4.37-4.42 (m, 1H); 4.19-4.25 (m, 1H); 4.07 (t, J = 6.7 Hz, 2H); 3.83 (s, 3H); 3.79 (s, 6); 2.83-2.98 (m, 2H); 2.73-2.80 (m, 4H); 2.55-2.64 (m, 2H); 2.46 (t, J = 6.8 Hz, 2H); 1.95-2.28 (m, 20H); 1.74-1.80 (m, 4H); 1.70 (s, 3H); 1.65 (s, 15H). ^{13}C-NMR ($CDCl_3$, 100 MHz): δ(ppm)= 125.2; 124.3 (2C); 109.8; 108.3 (2C); 107.00; 101.6; 73.8; 71.3; 64.3; 60.7; 56.2; 45.6; 43.8; 39.7 (2C); 38.7; 37.8; 37.7; 35.8; 33.1; 32.6 (2C); 28.3; 26.7; 26.0; 25.2; 24.5 (2C); 24.3; 24.1 (2C); 16.0 (5C). HPLC (CH_3CN) R_f 21 min; ESI-MS ($C_{57}H_{78}O_{11}S_2$): m/z 1025.6 $[M+Na]^+$. $[\alpha]^{22}_D$ = -51 (c = 0.900, $CHCl_3$).

13b: ^{1}H-NMR ($CDCl_3$, 400 MHz): δ(ppm)= 6.77 (s, 1H); 6.57 (s, 1H); 6.42 (s, 2H); 6.01 (d, J = 6.5 Hz, 2H); 5.91 (d, J = 9.0 Hz, 1H); 5.11-5.21 (m, 5H); 4.63 (d, J = 4.1 Hz, 1H); 4.39 (t, J = 7.8 Hz, 1H); 4.23 (t, J = 7.8 Hz, 1H); 4.06 (t, J = 6.7 Hz, 2H); 3.84 (s, 3H); 3.77 (s, 6H); 2.96 (dd, J = 9.0 Hz, J = 4.5 Hz, 1H); 2.79-2.90 (m, 1H); 2.30-2.47 (m, 16H); 1.52-1.78 (m, 24H); 1.35 (bs, 8H). ^{13}C-NMR ($CDCl_3$, 100 MHz, detected signals): δ(ppm)= 152.7; 135.0; 134.9; 132.4; 131.8; 128.5; 125.1; 124.4 (2C); 124.3 (2C); 109.8; 108.2 (2C); 107.0; 101.6 (2C); 73.4 (2C); 71.4; 64.0; 60.8; 56.2 (2C); 45.6; 43.8; 39.8 (3C); 38.8; 35.8; 34.4 (2C); 29.7; 29.1 (4C); 28.3 (3C); 27.0; 26.7 (2C);

25.0 (3C). HPLC (CH_3CN) R_f 23 min. ESI-MS ($C_{59}H_{82}O_{11}$): m/z 990.6 $[M+Na]^+$. $[\alpha]^{22}_D$ = -53 (c = 0.100, $CHCl_3$).

14a: ^{1}H-NMR ($CDCl_3$, 400 MHz): δ(ppm)= 8.42 (s, 1H); 8.25 (d, J = 8.0 Hz, 1H); 7.96 (d, J = 8.0 Hz, 1H); 7.86 (t, J = 8.0 Hz, 1H); 7.70 (t, J = 8.0 Hz, 1H); 7.24 (s, 1H); 5.70 (d, J = 17.2 Hz, 1H); 5.42 (d, J = 17.2 Hz, 1H); 5.31 (bs, 2H); 5.10-5.16 (m, 5H); 4.04 (t, J = 6.8 Hz, 2H); 2.61-2.76 (m, 6H); 2.40 (t, J = 7.3 Hz, 2H); 2.28- 2.33 (m, 1H); 2.15-2.20 (m, 1H); 1.98-2.09 (m, 22H); 1.62-1.76 (m, 20H); 1.00 (t, J = 7.5 Hz, 3H). ^{13}C-NMR ($CDCl_3$, 100 MHz): δ(ppm)= 173.6; 172.6; 168.2; 158.0; 153.0; 149.6; 147.0; 146.6; 135.8; 135.7; 134.3; 131.9; 131.4; 130.3; 129.2; 128.9; 128.7; 125.8; 125.0 (4C); 120.9; 96.6; 67.8; 64.9; 50.6; 40.4 (2C); 38.4; 37.9; 36.5; 33.3; 32.8; 32.5; 28.9 (2C); 27.6; 27.5 (2C); 26.4; 24.9; 24.6; 18.37; 16.7 (3C); 16.6; 8.3. HPLC (CH_3CN) R_f 27 min. ESI-MS ($C_{55}H_{72}N_2O_7S_2$): m/z 960.3 $[M+Na]^+$. $[\alpha]^{20}_D$ = -36 (c = 0.145, $CHCl_3$).

14b: ^{1}H-NMR ($CDCl_3$, 400 MHz): δ(ppm)= 8.42 (s, 1H); 8.24 (d, J = 8.0 Hz, 1H); 7.97 (d, J = 8.0 Hz, 1H); 7.86 (t, J = 8.0 Hz, 1H); 7.69 (t, J = 8.0 Hz, 1H); 7.24 (s, 1H); 5.70 (d, 16.0 Hz, 1H); 5.42 (d, J = 16.0 Hz, 1H); 5.31 (bs, 2H); 5.12-5.18 (m, 5H); 4.04(t, J = 7.5 Hz, 2H); 2.48-2.59 (m, 2H); 2.27-2.36 (m, 1H); 2.21-2.25 (m, 2H); 2.14-2.20 (m, 1H); 1.95-2.14 (m, 20H); 1.59-1.77 (m, 22H); 1.28 (bs, 8H); 1.00 (t, J = 8.1 Hz, 3H). ^{13}C-NMR ($CDCl_3$, 100 MHz, detected signals): δ(ppm)= 167.5; 146.0; 131.2; 130.6; 129.6; 128.5; 128.2; 128.0; 125.0; 124.4; 124.3; 120.4; 96.0; 67.1; 64.0; 49.9; 39.7; 35.8; 34.3; 33.8; 31.9; 29.7; 29.1; 29.0; 28.3; 26.9; 26.7; 25.7; 24.9; 24.6; 16.0; 7.6. HPLC (CH_3CN) R_f 28 min. ESI-MS ($C_{57}H_{76}N_2O_7$): m/z 924.2 $[M+Na]^+$. $[\alpha]^{20}_D$ = -21 (c = 0.175, $CHCl_3$).

15a: ^{1}H-NMR ($CDCl_3$, 400 MHz): δ(ppm)= 7.05 (s, 1H); 6.73 (s, 1H); 5.71 (dd, J = 11.4 Hz, J = 2.4 Hz, 1H); 5.55 (d, J = 7.9 Hz, 1H); 5.46 (d, J = 6.2 Hz, 1H); 5.37 (d, J = 7.1 Hz, 1H); 5.10-5.17 (m, 5H); 4.15-4.21 (m, 1H); 4.07 (t, J = 6.7 Hz, 2H); 3.28-3.44 (m, 1H); 3.00-3.11 (m, 1H); 2.89-

2.97 (m, 1H); 2.65-2.82 (m, 8H); 2.38-2.64 (m, 6H); 1.98-2.18 (m, 20H); 1.80-1.95 (m, 2H); 1.71-1.78 (m, 4H); 1.70 (s, 3H); 1.49-1.68 (m, 21H); 1.41 (s, 3H); 0.90-1.33 (m, 9H). ^{13}C-NMR ($CDCl_3$, 100 MHz, detected signals): δ(ppm)= 216.4; 172.9; 172.5; 170.6; 135.1; 135.0; 133.6; 125.2; 124.4; 75.8; 71.2; 64.3; 57.6; 57.3; 54.9; 54.4; 43.3; 42.5; 39.7; 38.5; 37.9; 37.6; 36.1; 35.8; 34.6; 32.7; 30.9; 29.7; 28.3; 26.9; 26.7; 25.7; 24.3; 23.9; 16.9; 16.0; 15.5. HPLC (CH_3CN) R_f 16 min. APCI-MS ($C_{61}H_{95}NO_9S_3$): m/z 1082.6 $[M]^+$. $[\alpha]^{22}_D$ = -7 (c = 0.100, $CHCl_3$).

15b: ^{1}H-NMR ($CDCl_3$, 400 MHz, detected signals): δ(ppm)= 7.05 (s, 1H); 6.75 (s, 1H); 5.72 (dd, J = 11.4 Hz, J = 2.5 Hz, 1H); 5.56 (dd, J = 9.9 Hz, J = 2.2 Hz, 1H); 5.44 (m, 1H); 5.36 (d, J = 7.4 Hz, 1H); 5.10-5.14 (m, 5H); 4.20 (m, 1H); 4.05 (t, J = 6.7 Hz, 2H); 3.34-3.40 (m, 1H); 3.05-3.09 (m, 1H); 2.90-2.94 (m, 1H); 2.82 (m, 2H); 2.50-2.72 (m, 5H); 2.28-2.38 (m, 6H); 2.97-3.18 (m, 20H); 1.55-1.80 (m, 20H); 0.98-1.47 (m, 26H). ^{13}C-NMR ($CDCl_3$, 100 MHz, detected signals): δ(ppm)= 173.9; 173.4; 170.6; 135.1; 135.0; 133.7; 125.1; 124.4; 75.8; 70.8; 64.0; 57.7; 54.9; 43.6; 39.8; 38.8; 37.5; 36.1; 35.8; 34.4; 31.6; 29.7; 29.1; 28.3; 26.9; 26.7; 25.7; 25.1; 25.0; 24.0; 22.7; 17.5; 16.1; 15.9; 15.6. HPLC (CH_3CN) R_f 17 min. ESI-MS ($C_{63}H_{99}NO_9S$): m/z 1069.4 $[M+Na]^+$. $[\alpha]^{20}_D$ = -20 (c = 0.080, $CHCl_3$).

4.1.7. Preparation of nanoassemblies (NAs)

In a standard procedure the nanoassemblies (NAs) were prepared by first dissolving the drug-squalene conjugates (Cs) in a volume of appropriate solvent (ethanol, acetone or THF). The solution was dropwise added under stirring (500 rpm) into a volume of MilliQ grade water. Finally, the organic solvent was completely evaporated using a Rotavapor® at 30°C under vacuum. The aqueous suspension of squalenoyl-drug nanoassemblies were stored at 5°C in the dark. To evaluate the optimal conditions to prepare stable nanoassemblies the influence of different variables to the process were considered: *A)* volume of solvent (500, 750 µL, 1 and 1.5 mL organic solvent) and a water volume of 1 mL and final concentration of 2 mg/mL; *B)* volume of water (500, 750 µL, 1,

1.5 and 2 mL) and a solvent volume of 500 µL, final concentration of 2 mg/mL; *C)* final drug-squalene conjugate concentration (0.5, 2, 4 mg/mL) in a final volume of 1 mL.; *D)* the ionic strength of water solution (10, 100 mM NaCl) in a volume of 1 mL and at 2 mg/mL ; *E)* the role of pH values (4.5, 7.2, 10.2) and buffer salts (acetate, citrate, phosphate, borate, carbonate) with a 500 µL of solvent, aqueous solution 1 mL at 2 mg/mL. The stability of NAs was evaluated by analyzing the mean particle size using a nanosizer, after incubation at 20°C for different times (zero, 24h, 48h) at a concentration of 0.2 mg/ml in water and 10 mM buffers: acetate pH 4.5, citrate pH 4.5, phosphate pH 7.2, borate pH 10.2, carbonate pH 10.2 .

4.1.8. Size and Zeta potential measurements

The average diameter and polydispersity index of the nanoassemblies was determined using quasi-elastic light scattering (QELS) at a fixed angle of 90°C and at a temperature of 25°C. The NAs dispersions were diluted 1:20 with MilliQ water before analysis. Each value reported is the average of five measurements. To determine the electrophoretic mobility, the NAs samples were diluted with 0.1 mM KCl and placed in the electrophoretic cell, where an electric field of 15.24 V/cm was established. Each sample was analyzed in triplicate. The zeta potential values were calculated using the Smolochowski equation.

4.1.9. Atomic force microscopy characterization.

AFM observation was done using a Park XE 100 atomic force microscope (Park Instruments, Sunnyvale, CA, USA). AFM images were obtained by measurement of the interaction forces between the tip (Mikromash NSC15) and the sample surface. The experiments were conducted at room temperature (20°C) and at atmospheric pressure (760 mmHg) operating in non-contact mode , in which the space between the tip and the sample is between 10 and 100 Å and the total force is very low. The resonant frequencies of this cantilever were found to be about 250 kHz. Immediately before the analysis, the samples were diluted in water (1:10 v/v) to obtain a less sticky fluid to

analyze. Droplets of constant volume (20 mL) of NAs were deposited onto a small mica disk with a diameter of 1 cm. After 2 min, excess water was removed using a paper filter.

In order to obtain stable and reproducible signals the NAs were prepared using 10 mM solution of NaCl, checking the QELS scattering intensity values to 700-900 Kcps for 0.2 mg/ml NAs preparation.

4.1.9. Stability assessment of drug-squalene conjugates (Cs) and nanoassemblies (NAs) in the presence of dithiothreitol (DTT), glutathione (GSH) and serum

The stability of NAs was evaluated by analyzing the mean particle size, after incubation at 20°C for different times (1h, 24h, 48h) at a concentration of 0.2 mg/ml in water and in 10 mM buffers: acetate pH 4.5, citrate pH 4.5, phosphate pH 7.2, borate pH 10.2, carbonate pH 10.2 .

Dithiothreitol (DTT): To define the stability of disulphide bonds inside compounds and NAs the method described by Satyam was essentially used, with slight modifications.[20] Each drug conjugates was dissolved in acetonitrile or ethanol/acetonitrile mixture to 1 mg/ml solution (0.5 ml) and were added 10 μl of borate buffer 0.2 M pH 9, 50 μl water and 20 μl of DTT (dissolved in acetonitrile) solution 16 mM. The vials were capped and kept at RT under nitrogen with occasional shaking by hand. For comparison the same solutions without DTT were prepared. Samples (20 μl) were spiked and analyzed by HPLC, as described above, at various time points. For evaluation of disulfide release data was considered the disappearance of the major peak related to the pure compound. The same proportions of buffer and DTT (dissolved in water) were used to analyze the stability of NAs. Samples kept at different times were diluted with acetonitrile (50 μl) just before HPLC injection. *Serum:* The stability of the conjugates was also analyzed in the presence of serum. Incubation in human serum was performed at 37°C with a final concentration of NAs of 0.33 mg/mL. Aliquots (60-80 μL) were removed after 48 h of incubation. After addition of 0.8 mL of acetonitrile, the aliquots were centrifuged and the solution was analyzed. All the tests were repeated

thrice. The chemical stability of the squalenoyl conjugates was determined by HPLC analysis. Samples in a range of 5-15 ug of the compounds were injected into a LiChrospher 100 RP 18e (4.6 × 250 mm, 5 μm) equipped with a C18 guard column. The column was eluted with acetonitrile / water (40:60 and, after 5 min, linear gradient to 100% acetonitrile, 35 min) at flow rate 1 mL/min, and the column effluent was detected at 227 nm for paclitaxel and camptothecin derivatives and 217 nm for podophyllotoxin and epothilone A derivatives. The assay was linear over the tested concentration range (1–50 μg as paclitaxel, podophyllotoxin, camptothecin and epothilone A). Eluted peaks were also characterized using a Waters HPLC-MS Micromass ZQ with ESI detector, eluting the column with methanol and 0.05% trifluoroacetic acid in water, with the same gradient as described above. *Glutathione (GSH):* (stability of compounds) a solution of GSH (0.0058 mmol) in H_2O (0.300 ml) was added to a solution of the squalene conjugate (0.0058 mmol) in MeOH (3 ml) and the reaction mixture was stirred at room temperature for 24 hours. A sample of the reaction mixture was submitted to an ESI-MS spectrometry analysis and in each case the peaks due to the free drugs were detected. (stability of compounds as NAs) incubation at 1 mg/ml with reduced glutathione (10 mM final concentration) at 37°C sampling the size of NAs after different times (0, 1, 6, 24, 48, 78 h). All the tests were repeated thrice.

4.1.10. Self-aggregation behavior of nanoassemblies

The critical aggregation concentration test (CAC) was performed by steady state fluorescence spectra as previously described.[6] Briefly: samples of the NAs in water, with concentrations ranging from 0.1 μg/L to 0.5 g/L, were incubated with a constant pyrene concentration of 6 x 10-7 M for 12h at room temperature under stirring. Fluorescence emission spectra were recorded from 360 to 550 nm, using 343 nm excitation wavelength. In the emission spectra of unstacked pyrene, the intensity ratio of the first band (I373) to the third band (I384) was analyzed as a function of NAs concentration. A CAC value was determined from the intersection of the tangent to the curve at the inflection with the horizontal tangent through the points at low concentration.

4.2. Biological assays

4.2.1. Cell cultures and fluorescence microscopy

Human lung carcinoma cell line A549 (CCL-185; American Type Culture Collection, Rockville, MD, USA) was grown in minimal essential medium with Earle's (E-MEM), supplemented with 10% fetal bovine serum (Hyclone Europe, Oud-Beijerland, Holland), 2 mM L-glutamine, 100 U/mL penicillin, and non-essential amino acids. Cells were maintained at 37°C in a humidified atmosphere at 5% CO_2. To test the ability of squalene bioconjugated to affect microtubule cytoskeleton, A549 cells (50000 cell/ml) were seeded on glass coverslips and grown in control medium. After 24 h, cells were incubated for 1 h with 200 μg/ml of the squalene bioconjugated, or with equal concentration of the parent compounds (paclitaxel, epothilone-A, podophyllotoxin). Cells were fixed and permeabilized for 6 min with methanol at -20°C, washed with PBS, and blocked in PBS+5% bovine serum albumin (BSA) for 15 min at room temperature. To localize tubulin, the cells were incubated with monoclonal anti-α-tubulin antibody (clone B-5–1–2, Sigma–Aldrich, St. Louis, MO) 1:500 in PBS for 1 h at 37°C. We used goat anti-mouse Alexa Fluor568 (Molecular Probes, Eugene, OR) 1:1000 in PBS+1% BSA for 45 min at 37°C as secondary antibodies. Nuclei staining was performed by incubation with DAPI (0.25 μg/mL in PBS) for 15 minutes at room temperature. The coverslips were mounted in Mowiol (Calbiochem, San Diego, CA)-DABCO (Sigma–Aldrich) and examined with a Zeiss Axiovert 200 microscope equipped with a 63x Neofluor lens (Zeiss, Oberkochen, Germany).

Furthermore, to ascertain that NA-**12a** is able to permeate cell membrane and bind microtubules, we removed unassembled tubulin, using previously described procedures[21] with minor modifications. With more detail, to avoid the administration of further paclitaxel, we used a microtubule-optimized PEM buffer (85 mM PIPES, pH 6.94, 10 mM EGTA, 1 mM $MgCl_2$, 2 M glycerol, 1 mM phenylmethylsulfonyl fluoride, 0.1 mM leupeptin, 1 μM pepstatin, 2 μg/ml aprotinin). After

fixation and permeabilization, cells were double immunostained using a polyclonal anti-taxol antibody (abcam, Cambridge, UK) 1:1000 in PBS for 1 h at 37°C and then a monoclonal anti-α-tubulin antibody. Afterward we used a mix of secondary antibodies, goat anti-mouse Alexa Fluor568 and donkey anti-rabbit Alexa Fluor488 (Life Technologies Italia, Monza, Italy). All other procedures were made as described above.

4.2.2. Cytotoxicity assay

The cytotoxicity assay of drug-squalene conjugates was carried out on MCF7 human breast cancer cell line and A549 human lung cancer. *MCF7*: Cell culture medium was used as dilution medium to make relevant dilutions of the nanoassemblies for this assay. Cytotoxicity was evaluated by incubating the cells with different concentrations of nanoassemblies for 48 h at 37 °C/5% CO_2. To evaluate the activity of NA after reduction of disulfides bridges, dithiotrithreitol was added to reach a 10 mM concentration and sample (at a 1 mM concentration) was incubated for 1h at 37°C. For comparison purposes, Paclitaxel, Podophyllotoxin , Camptothecin and Epothilone A were used as a control. In brief, MCF7 cells (25000/well) were cultured in RPMI 1640 supplemented with 10% fetal calf serum, 50 U/mL penicillin, 50 μg/mL streptomycin and 2 mM L-glutamine. The cytotoxicity of drugs and drug-squalene NAs was determined using sulforhodamine B (SRB) assay essentially as described by Voigt.[22] MCF-7 cells were seeded at a density of 25×10 3 cells/well in a 96 well plate and incubated for 24 h. Then various concentrations of drug-squalene NAs were added to the medium. After 48 h, the cell viability was determined by the SRB assay. Briefly, the medium was removed, and then cells were fixed with trichloroacetic acid, washed and stained with SRB (100 μl/well SRB 0,057% w/v in acetic acid 1% v/v). After washings 200 μl/well di Tris base 10 mM pH 10.5 were added and , after 30' the absorbance was measured at 492 nm using a 96-well plate reader (Titertek Multiskan PLUS MKII). The survival percentages were calculated using the following formula: Survival % = (A492 nm for the treated cells/A492 nm for the control cells) ×100%. The experiment was repeated thrice in triplicate for each concentration of the tested

compounds. Finally, dose–effect curves were made and IC 50 values were calculated. *A549*: The cytotoxicity of **12-15a** and **1-4** was evaluated also on A549 cells. Briefly, 25×10^2 cells/well in a 96 well plate and incubated for 24 h. Cells were then treated for 96hrs with different concentrations of nanoassemblies. Cytotoxic activity was evaluated by MTS and the IC50 calculated by interpolating the dose-response curve.

ACKNOWLEDGEMENTS

This research has been developed under the umbrella of CM1106 COST Action "Chemical Approaches for Targeting Drug Resistance in Cancer Stem Cells". The authors express their gratitude to Ettore Bernardi (Dep. Physic, Univ. degli Studi di Torino) for AFM experiments. A. Silvani thanks PRIN 2009 "Natural products and bioinspired molecules interfering with biological targets involved in control of tumor growth". The authors express their gratitude to Dr. Anna Daghetti (Dipartimento di Chimica, Università degli Studi di Milano) for her meticulous efforts in developing useful analytical methods for MS analysi and Ms. Ioana Stupariu for the revision of the manuscript.

REFERENCES

(1) Faraji, A. H., Wipf, P. (2009) Nanoparticles in cellular drug delivery *Bioorg. Med. Chem. 17*, 2950-2962.

(2) Liang, C., Yang, Y., Ling, Y., Huang, Y., Li, T., Li, X. (2011) Improved therapeutic effect of folate-decorated PLGA-PEG nanoparticles for endometrial carcinoma *Bioorg. Med. Chem. 19*, 4057-4066.

(3) Talekar, M., Kendall, J., Denny. W., Garg, S. (2011) Targeting of nanoparticles in cancer: drug delivery and diagnostic *Anti-Cancer Drugs 22*, 949-962.

(4) Hillaireau, H., Couvreur, P. (2009) Nanocarriers' entry into the cell: relevance to drug delivery *Cell. Mol. Life Sci. 66*, 2873-2896.

(5) Schroeder, U., Sommerfeld, P., Ulrich, S., Sabel, B. A. (1998) Nanoparticle technology for delivery of drugs across the blood-brain barrier *J. Pharm. Sci. 87*, 1305-1307.

(6) a) Dosio, F., Reddy, L. H., Ferrero, A., Stella, B., Cattel, L., Couvreur, P. (2010) Novel nanoassemblies composed of squalenoyl-paclitaxel derivatives: synthesis, characterization and biological evaluation *Bioconjugate Chem. 21*, 1349-1361; b) Caron, J., Maksimenko, A., Wack, S., Lepeltier, E., Bourgaux, C., Morvan, E., Leblanc, K., Couvreur, P., Desmaële, D. (2013) Improving the antitumor activity of squalenoyl-paclitaxel conjugate nanoassemblies by manipulating the linker between paclitaxel and squalene *Adv. Healthcare Mater. 2*, 172-185.

(7) Desmaële, D., Gref R., Couvreur P. (2012) Squalenoylation: A generic platform for nanoparticular drug delivery *Journal of Controlled Release 161*, 609-18.

(8) a) Maksimenko, A.; Mougin, J.; Mura, S.; Sliwinski, E.; Lepeltier, E.; Bourgaux, C.; Lepetre, S.; Zouhiri, F.; Desmaele, D.; Couvreur, P. (2013) Polyisoprenoyl gemcitabine conjugates self assemble as nanoparticles, useful for cancer therapy *Cancer Lett. 334,* 346 – 353. b) Couvreur, P., Stella, B., Reddy, L. H., Hillaireau, H., Dubernet, C., Desmaële, D., Lepêtre-Mouelhi, S., Rocco, F., Dereuddre-Bosquet, N., Clayette, P., Rosilio, V., Marsaud, V., Renoir, J. M., Cattel, L. (2006) Squalenoyl nanomedicines as potential therapeutics *Nano Lett. 6*, 2544-2548. c) Reddy, L. H., Khoury, H., Paci, A., Deroussent, A., Ferreira, H., Dubernet, C., Declèves, X., Besnard, M., Chacun, H., Lepêtre-Mouelhi, S., Desmaële, D., Rousseau, B., Laugier, C., Cintrat, J. C., Vassal, G., Couvreur, P. (2008) Squalenoylation favorably modified the in vivo pharmakokinetics and biodistribution of gemcitabine in mice *Drug Metabolism and Disposition 36*, 1570-1577.

(9) Sémiramoth N., Di Meo C., Zouhiri F., Saïd-Hassane F., Valetti S., Gorges R., Nicolas V., Poupaert J.H., Chollet-Martin S., Desmaële, D., Gref R., Couvreur P. (2012) Self-assembled squalenoylated penicillin bioconjugates: An original approach for the treatment of intracellular infections *ACS Nano 6*, 3820-31.

(10) Sarpietro M.G., Micieli D., Rocco F., Ceruti M., Castelli F. (2009) Conjugation of squalene to acyclovir improves the affinity for biomembrane models *International Journal of Pharmaceutics 382*, 73-9.

(11) Allain V., Bourgaux C., Couvreur P. (2012) Self-assembled nucleolipids: From supramolecular structure to soft nucleic acid and drug delivery devices *Nucleic Acids Research 40*, 1891-903.

(12) Raouane M., Desmaële D., Gilbert-Sirieix M., Gueutin C., Zouhiri F., Bourgaux C., Lepeltier, E., Gref R., Ben Salah R., Clayman G., Massaad-massade L., Couvreur P. (2011) Synthesis, characterization, and in vivo delivery of siRNA-squalene nanoparticles targeting fusion oncogene in papillary thyroid carcinoma *Journal of Medicinal Chemistry 54*, 4067-76.

(13) Arias J.L., Reddy L.H., Othman M., Gillet B., Desmaële D., Zouhiri F., Dosio F., Gref R., Couvreur P. (2011) Squalene based nanocomposites: A new platform for the design of multifunctional pharmaceutical theragnostics *ACS Nano 5*, 1513-21.

(14) Dosio F., Stella B., Ferrero A., Garino C., Zonari D., Arpicco S., Cattel L., Giordano S., Gobetto R. (2013) Ruthenium polypyridyl squalene derivative: A novel self-assembling lipophilic probe for cellular imaging *International Journal of Pharmaceutics 440*, 221-8.

(15) *Synthesis of tubulin binders:* (a) Calogero, F.; Borrelli, S.; Speciale, G.; Christodoulou, M. S.; Cartelli, D.; Ballinari, D.; Sola, F.; Albanese, C.; Ciavolella, A.; Passarella, D.; Cappelletti, G.; Pieraccini, S.; Sironi, M. (2013) 9-Fluorenone-2-carboxylic acid as scaffold for new tubulin interacting compounds *ChemPlusChem*, *78*, 663-9; (d) Riva, E.; Mattarella, M.; Borrelli, S.; Christodoulou, M. S.; Cartelli, D.; Main, M.; Faulkner, S.; Sykes, D.; Cappelletti, G.; Snaith, J. S.; Passarella, D. (2013) reparation of Fluorescent Tubulin Binders *ChemPlusChem* P *78*, 222; (o) Passarella, D.; Comi, D.; Cappelletti, G.; Cartelli, D.; Gertsch, J.; Quesada, A. R.; Borlak, J.; Altmann, K.-H. (2009) Synthesis and biological evaluation of epothilone A dimeric compounds *Bioorg. Med. Chem. 17*, 7435-40; (q) Passarella, D.; Giardini, A.; Peretto, B.; Fontana, G.; Sacchetti, A.; Silvani, A.; Ronchi, C.; Cappelletti, G.; Cartelli, D.; Borlak, J.; Danieli, B. (2008) Inhibitors of tubulin polymerization: Synthesis and biological evaluation of hybrids of vindoline, anhydrovinblastine and vinorelbine with thiocolchicine, podophyllotoxin and baccatin III *Bioorg. Med. Chem. 16*, 6269-85.

(16) *Synthesis of topoisomerase inhibitors:* (e) Christodoulou, M. S.; Zunino, F.; Zuco, V.; Borrelli, S.; Comi, D.; Fontana, G.; Martinelli, M.; Lorens, J. B.; Evensen, L.; Sironi, M.; Pieraccini, S.; Dalla Via, L.; Gia, O. M.; Passarella, D. (2012) Camptothecin-7-yl-methanthiole: Semisynthesis and Biological Evaluation *ChemMedChem 7*, 2134-43.

(17) *Synthesis of Tyrosine Kinases inhibitors:* (c) Peruzzotti, C.; Borrelli, S.; Ventura, M.; Pantano, R.; Fumagalli, G.; Christodoulou, M. S.; Monticelli, D.; Luzzani, M.; Fallacara, A. L.; Tintori, C.; Botta, M.; Passarella, D. (2013) Probing the Binding Site of Abl Tyrosine Kinase Using in Situ Click Chemistry *ACS Med. Chem. Lett. 4*, 274; (f) Colombo, F.; Tintori, C.; Furlan, A.; Borrelli, S.; Christodoulou, M. S.; Dono, R.; Maina, F.; Botta, M.; Amat, M.; Bosch, J.; Passarella, D.; (2012) Click'synthesis of a triazole-based inhibitor of Met functions in cancer cells *Bioorg. Med. Chem. Lett. 22*, 4693; (h) Furlan, A.; Colombo, F.; Kover, A.; Issaly, N.; Tintori, C.; Angeli, L.; Leroux, V.; Letard, S.; Amat, M.; Asses, Y.; Maigret, B.; Dubreuil, P.; Botta, M.; Dono, R.; Bosch, J.; Piccolo, O.; Passarella, D.; Maina, F. (2012) Identification of new aminoacid amides containing the imidazo[2,1-b]benzothiazol-2-ylphenyl moiety as inhibitors of tumorigenesis by oncogenic Met signalling *Eur. J. Med. Chem. 47*, 239; (k) Arioli, F.; Borrelli, S.; Colombo, F.; Falchi, F.; Filippi, I.; Crespan, E.; Naldini, A.; Scalia, G.; Silvani, A.; Maga, G.; Carraro, F.; Botta, M.; Passarella D. (2011) *N*-[2-Methyl-5-(triazol-1-yl)phenyl]pyrimidin-2-amine as a Scaffold for the Synthesis of Inhibitors of Bcr-Abl *ChemMedChem 6*, 2009;

(18) *Synthesis of miscellaneous inhibitors:* (b) Christodoulou, M. S.; Fokialakis, N.; Passarella, D.; García-Argáez, A. N.; Gia, O. M.; Pongratz, I.; Lisa Dalla Via, L.; Haroutounian, S. A. (2013) Synthesis and biological evaluation of novel tamoxifen analogues *Bioorg. Med. Chem. 21*, 4120-31; (g) Christodoulou, M. S.; Colombo, F.; Passarella, D.; Ieronimo, G.; Zuco, V.; De Cesare, M.; Zunino, F. (2011) Synthesis and biological evaluation of imidazolo[2,1-b]benzothiazole derivatives, as potential p53 inhibitors *Bioorg. Med. Chem. 19*, 1649;

(19) *Synthesis of disulfide containing compounds:* (j) Cappelletti, G., Cartelli, D., Peretto, B., Ventura, M., Riccioli, M., Colombo, F., Snaith, J. S., Borrelli, S., Passarella, D. (2011), Tubulin-

guided dynamic combinatorial library of thiocolchicine-podophyllotoxin conjugates *Tetrahedron 67*, 7354-7357; (l) Passarella, D., Peretto, B., Blasco y Yepes, R., Cappelletti, G., Cartelli, D., Ronchi, C., Snaith, J. S., Fontana, G., Danieli, B., Borlak, J. (2010) Synthesis and biological evaluation of novel thiocolchicine-podophyllotoxin conjugates *Eur. J. Med. Chem. 45*, 219-226; (p) Passarella, D.; Comi, D.; Vanossi, A.; Paganini, G.; Colombo, F.; Ferrante, L.; Zuco, V.; Danieli, B.; Zunino, F. (2009) Histone Deacetylase and Microtubules as Targets for the Synthesis of Releasable Conjugate Compounds *Bioorg. Med. Chem. Lett. 19*, 6358; (n) Riva, E., Comi, D., Borrelli, S., Colombo, F. Danieli, B., Borlak, J., Evensen, L., Lorens, J. B., Fontana, G., Gia, O. M., Dalla Via, L., Passarella, D. (2010) Synthesis and biological evaluation of new camptothecin derivatives obtained by modification of position 20 *Bioorg. Med. Chem. 18*, 8660-8668;

(20) Satyam, A. (2008) Design and synthesis of releasable folate-drug conjugates using a novel heterobifunctional disulfide-containing linker. *Bioorg. Med. Chem. Letters*. *18,* 3196-3209

(21) Cappelletti, G., Tedeschi, G., Maggioni, M.G., Negri, A., Nonnis, S., Maci, R. (2004) The nitration of τ protein in neurone-like PC12 cells *FEBBS 562,* 35-39.

(22) Voigt W. (2005) Sulforhodamine B assay and chemosensitivity *Methods in molecular medicine 110*, 39-48.

(23) Blencowe, C. A., Russel, A. T., Greco, F., Hayes, W., Thornthwaite, D. W. (2011) Self-immolative linkers in polymeric delivery systems *Polym. Chem. 2*, 773-790.

(24) Ceruti M., Balliano G., Viola F., Cattel L., Gerst N., Schuber F. (1987) Synthesis and biological activity of azasqualenes, bis-azasqualenes and derivatives *Eur. J. Med. Chem. 22*, 199-208.

(25) Zhao Z., Kingston D.G.I., Crosswell A.R. (1991) Modified taxols, 6. Preparation of water-soluble prodrugs of taxol J Nat Prod. 54, 1607-11.